



Characterisation of Artificial and Natural Defects in Fibre Reinforced Plastics Designed for Energy Applications Using Active Thermography

Christiane MAIERHOFER¹, Rainer KRANKENHAGEN¹, Mathias RÖLLIG¹,
Stefanie RIEMER¹, Michael GOWER², Graham BAKER², Maria LODEIRO²,
Lenka KNAZOVICKÁ³, Ales BLAHUT³, Christian MONTE⁴, Albert ADIBEKYAN⁴,
Berndt GUTSCHWAGER⁴

¹ Federal Institute for Materials Research and Testing (BAM), Berlin, Germany

² National Physical Laboratory, Teddington, Middlesex, UK

³ CMI OI Praha, Praha 10, Czech Republic

⁴ Physikalisch-Technische Bundesanstalt (PTB), Berlin, Germany

Contact e-mail: christiane.maierhofer@bam.de

Abstract. Amongst various other NDT methods, within the EMRP-project 'VITCEA' active thermography is validated for testing of CFRP and GFRP structures constructed for energy application. In this contribution, the optical and thermal properties of CFRP and GFRP reference defect artefact (RDA) and natural defects artefact (NDA) test specimens are characterized. Different excitation techniques and techniques for data analysis are compared for optimizing the number of detected defects.

1. Introduction

The increased use of fibre-reinforced plastic (FRP) composites for improved efficiency and reliability in energy related applications e.g. wind and marine turbine blades, nacelles, oil and gas flexible risers, also increases the demand for innovative non-destructive testing (NDT) technologies. The early, reliable and accurate detection of complex defects is a challenge for complementary NDT techniques. Thus, in order to achieve increased acceptance of suitable and optimised NDT methods by industry, the European Metrology Research Programme (EMRP) project ENG57 Validated Inspection Techniques for Composites in Energy Applications (VITCEA) deals with the development and validation of innovative NDT technologies [1]. In this project, four NDT methods were further developed, applied to selected fibre-reinforced plastic (FRP) composite materials containing various kinds of defects, and compared to each other. These NDT methods include scanning techniques (microwave and ultrasonics), and non-contact, full-field methods (active thermography and shearography). In this paper, only the results concerning the validation of active thermography are presented.

As a first objective in the project, a large number of test specimens with artificial defects (reference defect artefacts, RDA) and with natural defects (natural defect artefacts, NDA) were designed and manufactured. The materials used for the construction of RDAs



and NDAs were glass and carbon fibre based thermoset (epoxy) and thermoplastic (polyamide-12) composites of various lay-ups including unidirectional, cross-ply and quasi-isotropic stacking sequences. Flat bottom drilled holes, simulated delaminations constructed from thin PTFE film and Kapton tape and regions of intentional in-plane fibre misalignment were included as artificial defects. Natural defects (e.g. delaminations, matrix cracking etc) were generated by machining notches into rectangular coupons which were then loaded in tension until the onset of damage. Other NDAs were created by low velocity impact at different energy levels mainly in accordance with ASTM D7136 [2].

For an appropriate comparison of experimental and numerical data of active thermography, optical properties such as emissivity and transmissivity were determined with high accuracy as a function of angle (directional), wavelength (spectral) and temperature. Additionally, the thermal conductivity and diffusivity will, in ongoing work, be evaluated in all three principal material directions (i.e. two in-plane and one out-of-plane directions). Measurements using active thermography were performed on coupons of material used for the creation of NDAs before damage to obtain reference data and to look for the presence of unintentional defects. The artificial and natural defects were investigated and were characterized related to their lateral geometry, thermal properties and coverage. Different thermal excitation methods are compared. The main innovation of these investigations is to obtain defect information with the highest accuracy and resolution by using well characterised material properties in combination with optimised data analysis procedures. Selected results concerning the determination of optical properties (emissivity and transmissivity), the comparison of different excitation methods (flash, step and lockin excitation) and of methods for data analysis (thermal contrast and pulse-phase-thermography) for inspection of defects in CFRP and GFRP materials are presented below.

2. Test specimens

2.1 Reference defect artefact (RDA) test specimens

The three RDA test laminates used in this study were designed and constructed according to the drawing in Figure 1. Each RDA contains 12 artificial delaminations with diameters of 3, 6, 12, and 25 mm, 9 regions of 15° in-plane fibre deviations (deviation with respect to the parent ply orientation) with sizes of 6, 12, and 25 mm square, 9 drilled holes with diameters of 1, 2, and 3 mm and three hole arrays consisting of 3 x 3 holes in close formation, each hole having a diameter of 1 mm.

Table 1. Material properties of the RDA and NDA test specimens

Material	Detail	Number of layers and orientation	Diffusivity in cm^2/s ¹	Test specimen
CFRP	Gurit SE84LV carbon fibre epoxy UD prepreg, T700 fibre	16 ply UD lay-up (total thickness of ~5.2 mm)	0.0039 ± 0.0002	RDA 1a_r RDA 1a_s
CFRP	Gurit SE84LV carbon fibre epoxy UD prepreg T700 fibre	8 and 16 ply QI lay-up [+45/0/-45/90] _{2s} (total thickness of ~2.5 and 5 mm)	0.0039 ± 0.0002	NDA_AFMF NDA_1AFMG NDA_2AFMG
GFRP	913 epoxy E-glass fibre reinforced UD prepreg	20 ply cross-ply [0/90] _{10s} lay-up (total thickness of ~5.8 mm)	0.0027 ± 0.0002	RDA 2a
GFRP	MTM 28 epoxy resin black pigmented glass fibre system	40 layers [+45/0/-45/90] _{5s} lay-up (total thickness of ~6 mm)	0.0031 ± 0.0002	NDA_2AFSN

¹Diffusivity in the out-of-plane direction, determined experimentally from active thermography measurements in transmission configuration with flash excitation.

For all defect types the through-thickness positions included: (i) near the front face (material coverage of ~ 0.6 mm), (ii) mid-thickness (coverage of ~ 2.4 mm), and (iii) near the back face (coverage of ~ 4.2 mm).

Two of the test specimens were made from SE84 CFRP, one having a rough, matt surface (RDA 1a_r) and the other a smooth, glossy surface (RDA 1a_s). Both CFRP RDAs were of unidirectional (UD) lay-up and had a thickness of 5.2 mm. The third test specimen was made from 913 GFRP (RDA 2a), and was slightly translucent in the visual wavelength range (see photo in Figure 1.b), has a glossy surface, fibre orientations of $0^\circ/90^\circ$ (cross-ply) and a thickness of 5.8 mm.

All three RDAs were processed in an autoclave with documented temperature and pressure profiles. The material parameters of the CFRP and GFRP laminates are summarized in table 1. Here, the diffusivity of the materials in the out-of-plane direction was determined from transmission measurements with flash excitation as outlined in [3]. For RDAs 1a_s and _r, no blackening of the surface was required, while test specimen RDA 2a was inspected with and without blackening of both surfaces.

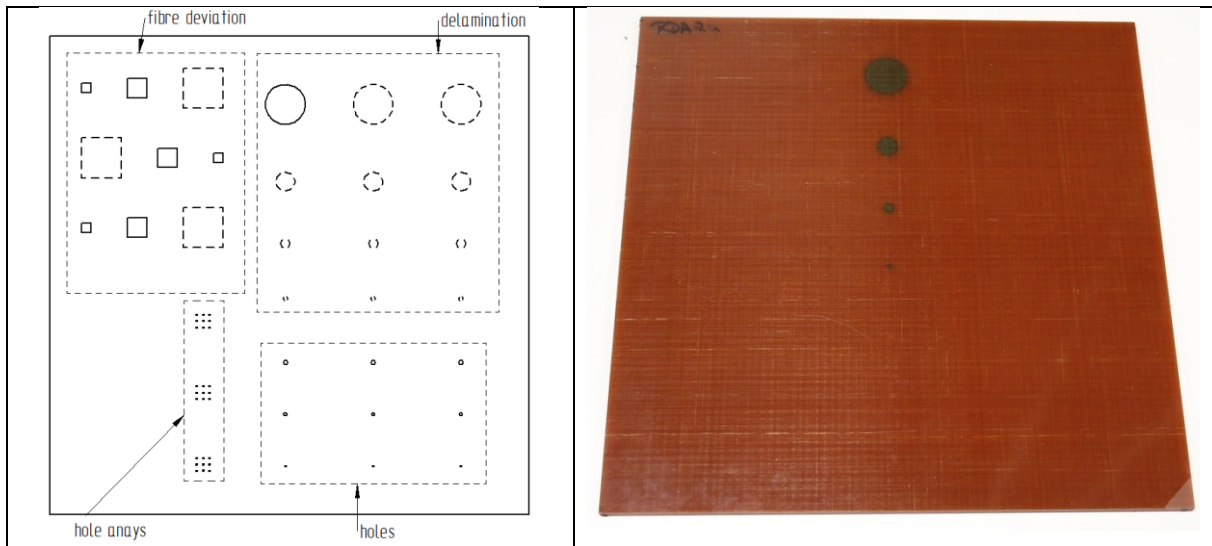


Fig. 1. a) Drawing of the position of the artificial defects in all RDA test specimens. The size of the test specimens is 280 x 280 mm. b) Photo of RDA 2a made of GFRP is partially translucent in the visible wavelength range. The delaminations close to the surface could be seen directly in the photo.

2.2 Natural defect artefact (NDA) test specimens

For the NDA test specimens, quasi-isotropic CFRP coupons with thicknesses of 2.5 and 5 mm and several GFRP coupons comprising of different matrix systems (two types of epoxy and one thermoplastic (PA12)) and thicknesses were constructed. For the CFRP plates discussed in the following (NDA_AFMF, NDA_1AFMG, NDA_2AFMG), the same prepreg material was used as for RDA 1a, but with a quasi-isotropic (QI) lay-up, see Table 1. For the GFRP material mentioned below, a black pigmented epoxy resin system was used, see again Table 1. Each of the plates was cut into nine pieces. Some of these pieces were damaged with impact loads and some with tensile loads. For the impact loads, low velocity impacts with energies between 1 and 16 J were imparted using a drop weight tower with a hemispherical steel indenter with a diameter of 12 mm. For the tensile load, a testing machine with a maximum tensile load of 100 kN was used. Before loading, notches were cut at the middle of the rectangular pieces of the plate with depths of 1.25 and 2.5 mm (bottom of the notches was positioned in the middle of the 2.5 and 5 mm thick coupons) and 4 mm (deep notch in the 5 mm thick plate).

3. Characterisation of optical properties

3.1 Experimental set-up

Additional test samples of the CFRP Gurit SE84LV and GFRP MTM 28 without defects with a thickness of 5 mm were fabricated to investigate the optical properties of the materials. The transmittances and emissivities of the materials are required for the calculation of the radiation transport within the sample and the numerical simulation of the active thermography experiments. In a first step the materials were investigated for residual transmittance. Subsequently the emissivities of the non-transparent opaque samples were determined at PTB's emissivity setup in air. The setup is described in detail elsewhere [5]. Briefly, the spectral radiances of the samples at a specific temperature are measured with respect to the spectral radiance of a blackbody at known temperature. The samples are mounted in a temperature controlled hemispherical enclosure with known emissivity of the interior walls. By knowing the temperatures of samples, enclosure, blackbody and spectrometer the directional spectral emissivities of the samples can be determined from the measurements. Directional spectral measurements at angles from 10° to 70° were performed at sample temperature of 25° in the wavelength range from $5\ \mu\text{m}$ to $25\ \mu\text{m}$.

3.2 Results

The directional spectral emissivities of GFRP MTM28 recorded under angles of observation from 10° to 70° are shown in Figure 2. An overall emissivity of about 0.95 at near normal observation and a typical decrease to lower values at larger angles of observation is found.

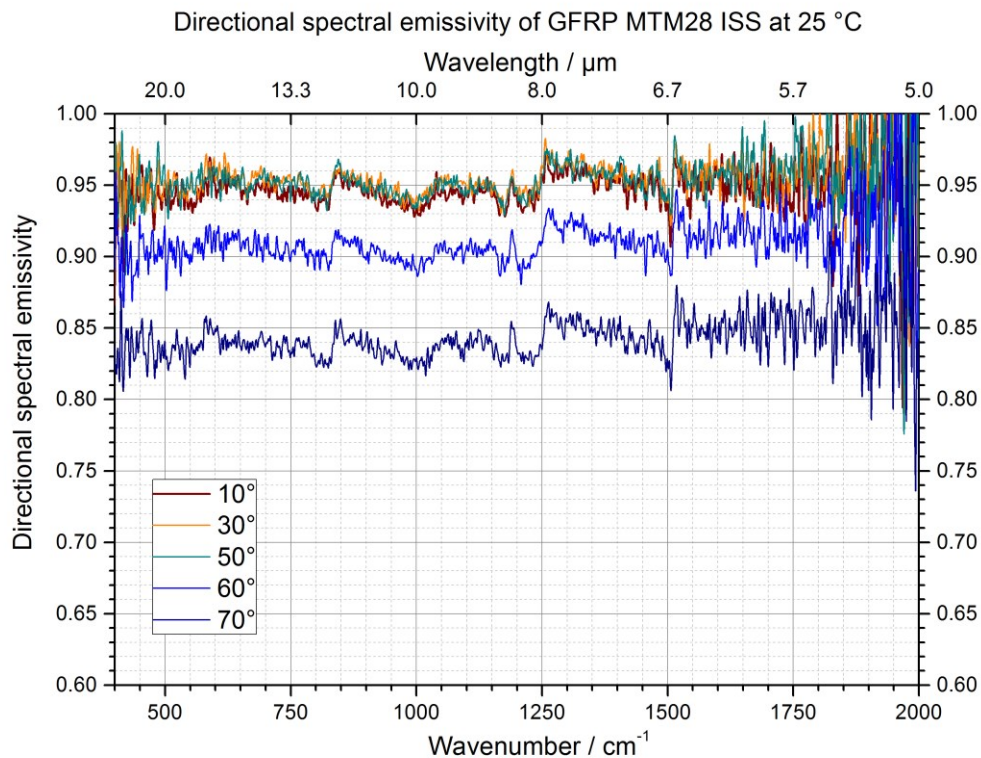


Fig. 2. Directional spectral emissivity of GFRP MTM28 determined at 25°C under angles of observation from 10° to 70° .

The directional spectral emissivity of CFRP SE84LV shown in Figure 3 is slightly lower ranging from 0.83 to 0.94 for near normal observation but also decreasing towards larger angles of observation.

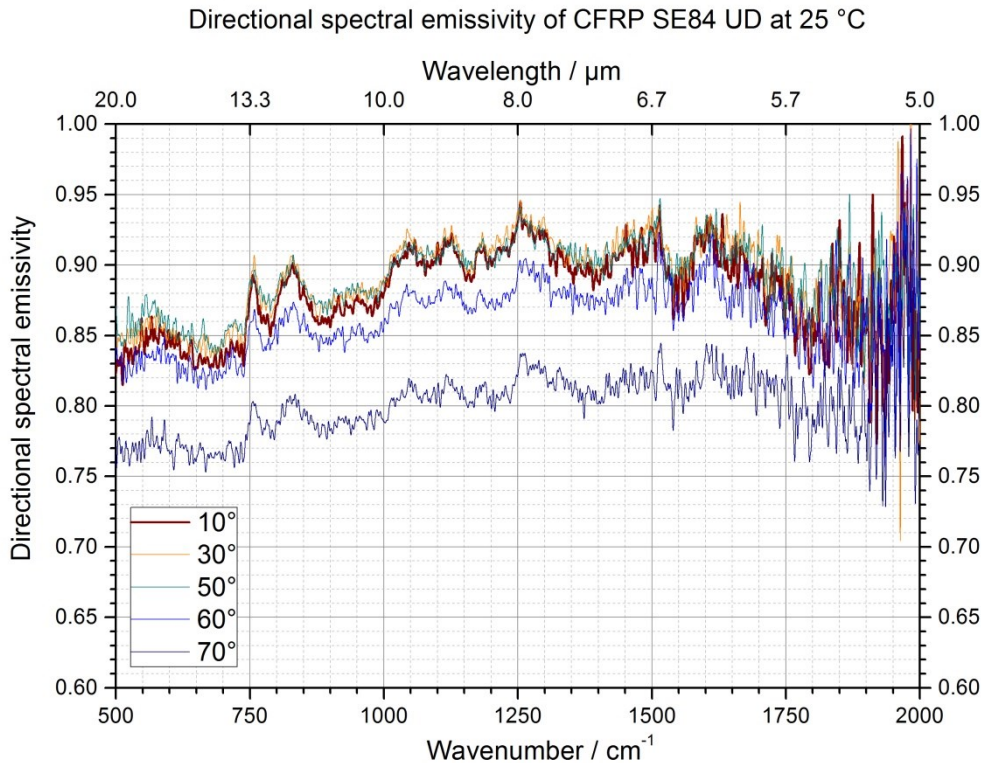


Fig. 3. Directional spectral emissivity of CFRP SE84 determined at 25 °C under angles of observation from 10° to 70°.

4. Active thermography inspection of RDAs

4.1 Experimental set-up

The RDA test specimens were investigated with active thermography using three different techniques of excitation: flash excitation, lockin excitation and step excitation with an IR radiator. For all techniques, measurements were performed in reflection configuration, where the heating source and the IR camera were positioned at the front side of the test specimen (side where the holes are not visible). For flash and step excitation, measurements in transmission configuration were also made. For each technique, the parameters are summarized in Table 2. The data were recorded at frame rates between 10 and 50 Hz and with a sequence length of 3000 frames.

For data analysis, first of all the so-called zero thermogram (thermogram recorded before heating) was subtracted from the whole sequence. Subsequently, thermograms and averaged thermograms having an optimum contrast of the defects were selected. Additionally, all sequences were analysed by applying pulse-phase-thermography [4] to the data recorded during cooling down. For lockin excitation, 14 periods were analysed by skipping the first 5 periods of the sequence. Amplitude and phase images were calculated at 0.02 Hz. As for all cases the phase images show a similar number of defects or more than the thermograms, only the phase images are displayed in Figure 4.

Table 2. Heating and measurement parameters for the RDA and NDA test specimens.

Heat source	Total power/energy consumption	Duration of heating in s	Configuration	IR camera
4 flash lamps	24 kJ (1.7 J/cm ²) ¹	2.4 ms	reflection and transmission	InSb FPA, 2 to 5 μm, 1240x1024 pixels
2 halogen lamps	4200 W	1000 s at 0.02 Hz	reflection	MCT FPA, 640x512 pixels
1 IR radiator	2400 W	15 s	reflection and transmission	InSb FPA, 2 to 5 μm, 1240x1024 pixels

¹ Energy density measured at the position of the test specimen.

4.2 Results

The phase images shown in Figure 4 were recorded at those frequencies, where most of the defects could be detected. From these data, the following observations could be made:

- The fibre deviation defects could not be detected.
- For all test specimens, most of the defects could be detected with step excitation in reflection configuration. All defects close to the surface and in the middle of the plate (despite the single 1 mm holes) were found.
- Two of the largest delaminations located close to the back face were only visible with step excitation in transmission configuration in the GFRP RDAs.
- In the CFRP test specimens (RDA 1a_r and RDA 1a_s), more signatures related to unintentional defects are visible.
- In the CFRP test specimens, the signatures of the defects are slightly elongated in horizontal direction, which is the orientation of the UD fibres.

Thus, it can be concluded that the most artificial defects could be detected in GFRP by using step heating with an IR radiator. In GFRP, the signature of the defects is sharper than in CFRP, as in CFRP the in-plane thermal diffusivity is higher resulting in a blurring of the defects in fibre direction. In reflection configuration, the maximum penetration depth reaches the middle of the plate. Few of the defects located close to the back face could only be detected in transmission configuration.

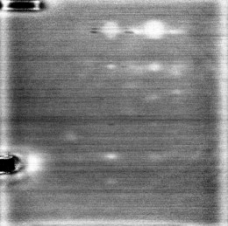
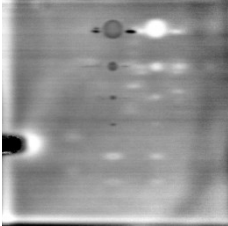
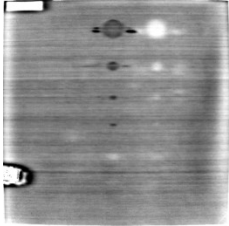
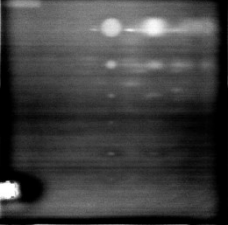
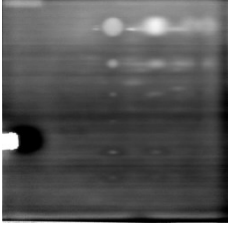
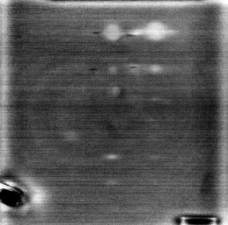
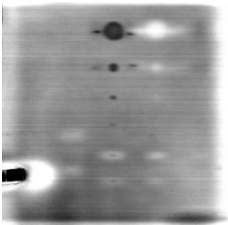
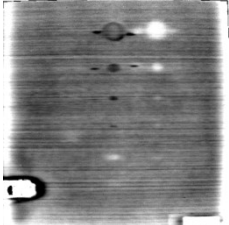
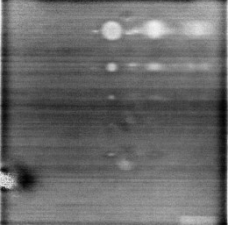
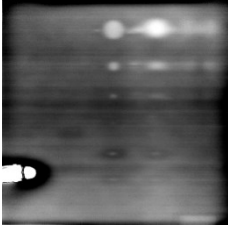
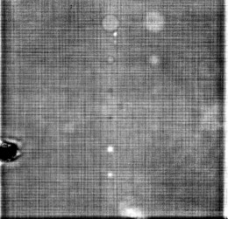
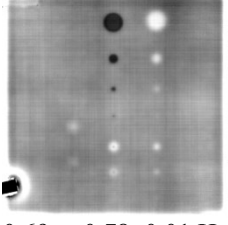
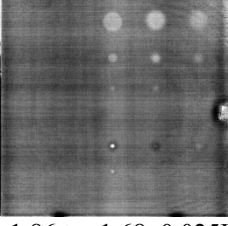
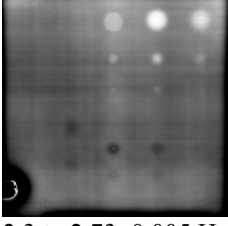
Test specimen	Configuration	Flash Excitation	Step excitation	Lockin excitation
RDA 1a_r	Reflection	 0.47 to 0.55; 0.02 Hz	 0.95 to 1.05; 0.02 Hz	 1.36 to 1.44; 0.02 Hz
	Transmission	 2.45 to -2.27; 0.02 Hz	 -2.2 to -2.0; 0.02 Hz	-
RDA 1a_s	Reflection	 0.49 to 0.57; 0.02 Hz	 0.81 to 0.9; 0.02 Hz	 1.37 to 1.43; 0.02 Hz
	Transmission	 -1.95 to -1.78; 0.04 Hz	 -2.62 to -2.43; 0.02 Hz	-
RDA 2a	Reflection	 0.61 to 0.68; 0.02 Hz	 0.69 to 0.78; 0.01 Hz	-
	Transmission	 -1.86 to -1.68; 0.025Hz	 2.3 to 2.73; 0.005 Hz	-

Fig. 4. Phase images calculated from the sequences which were recorded with different types of excitation in two different configurations (reflection and transmission) at the three RDA test specimens. The numbers below the images are giving the minimum and maximum phase angles in rad of the images related to a linear grey scale from black to white, respectively.

5. Experiments at NDAs

Up to now, only flash excitation has been applied to the NDA test specimens. Here, measurements in reflection configuration were obtained from the front as well as from the back face. In Figure 5, only thermograms and phase images recorded from the back face (opposite site of the impact and of the notch) are shown.

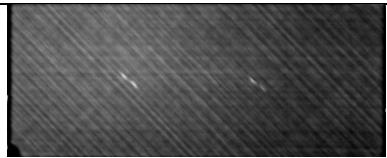
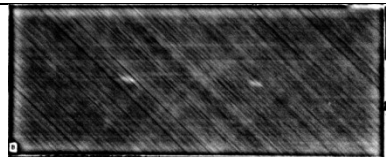
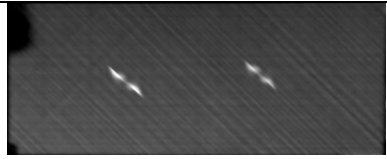
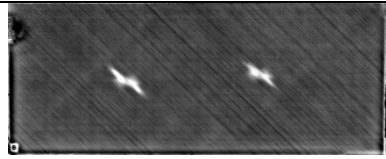

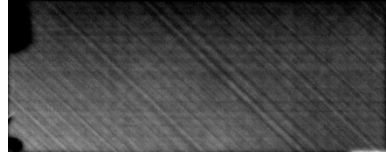
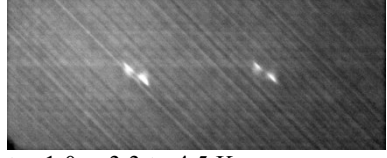
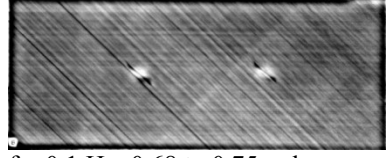
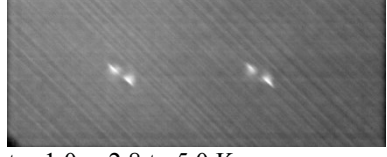
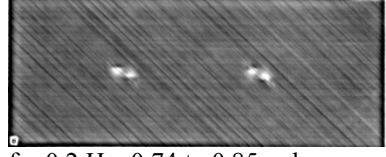

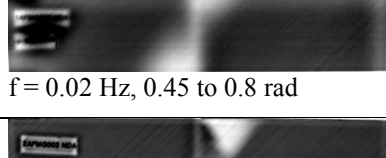
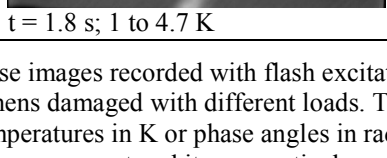
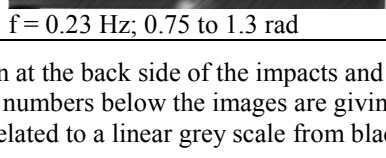
NDA	Damage	Thermogram	Phase image
AFMF_001 2.5 mm thick	Impact 2 J	 t = 0.56 s; 4.6 to 6.5 K	 f = 0.2 Hz; 0.7 to 0.76 rad
AFMF_002 2.5 mm thick	Impact 4 J	 t = 0.42 s; 4 to 10 K	 f = 0.2 Hz; 0.52 to 0.67 rad
2AFMG_002 5 mm thick	Impact 3.4 J	 t = 1.0 s; 3.3 to 4.5 K	 f = 0.1 Hz; 0.68 to 0.75 rad
2AFMG_001 5 mm thick	Impact 6.8 J	 t = 1.0 s; 3.3 to 4.5 K	 f = 0.1 Hz; 0.68 to 0.75 rad
1AFMG_008 5 mm thick	Impact 8 J	 t = 1.0 s; 2.8 to 5.0 K	 f = 0.2 Hz; 0.74 to 0.85 rad
1AFMG_005 5 mm thick notch in the middle	Tensile load, failure at 0.258 GPa	 t = 13.5 s; 0.6 to 1.4 K	 f = 0.02 Hz; 0.45 to 0.8 rad
2AFMG_003 5 mm thick deep notch	Tensile load, failure at 0.366 GPa	 t = 1.8 s; 1 to 4.7 K	 f = 0.23 Hz; 0.75 to 1.3 rad

Fig. 5. Thermograms and phase images recorded with flash excitation at the back side of the impacts and notches of the NDA test specimens damaged with different loads. The numbers below the images are giving the minimum and maximum temperatures in K or phase angles in rad related to a linear grey scale from black to white, respectively.

Here, the following observations can be summarized:

- The areas of damage appear larger in the phase images, which might be explained with the higher penetration depth of these.
- As expected, the impact damage increases with decreasing plate thickness (for a given impact energy level) and with increasing energy.
- The delamination in the tensile loaded specimen, with the notch extended to mid-thickness (1AFMG_005) appears at only one depth and extends symmetrically about

- the notch.
- The delamination of the tensile loaded test specimen with the deep notch (2AFMG_003) is appearing at two depths and is mainly extended to only one side of the notch.

6. Conclusion and outlook

In summary, first RDA and NDA test specimens were designed, fabricated and characterisation of optical and thermal properties undertaken. Secondly, active thermography was applied with different excitation techniques. Most of the RDA defects could be detected using step excitation and data analysis based on pulse-phase-thermography. In GFRP, more defects could be detected than in CFRP, which could be related to the higher anisotropy of the thermal properties in CFRP due to the orientation of the carbon fibres.

In the future, further excitation techniques such as chirp signals and step heating with halogen lamps will be applied and further data analysis techniques like thermal signal reconstruction will be evaluated. Detailed studies will be based on the analysis of the signal to noise ratio. Finally, more RDA and NDA test specimens will be analysed.

Acknowledgements

This work was part of the ENG57 VITCEA-project in the European Metrology Research Programme (EMRP) funded by EURAMET / NMS. We gratefully acknowledge the support of B. Rehmer from BAM 5.2 for the realisation of the tensile load tests and of Block GmbH for the insertion of the impacts. S. Augustin was involved in the documentation of the investigation of the tensile loaded samples.

References

- [1] ENG57 VITCEA - Validated Inspection Techniques for Composites in Energy Applications. <http://projects.npl.co.uk/vitcea/> EMRP-Project
- [2] ASTM D7136 – 2015 Standard Test Method for Measuring the Damage Resistance of a Fiber-Reinforced Polymer Matrix Composite to a Drop-Weight Impact Event
- [3] Maierhofer, C., Myrach, P., Reischel, M., Steinfurth, H., Röllig, M., Kunert, M. Characterizing damage in CFRP structures using flash thermography in reflection and transmission configurations. *Composites: Part B* 57 (2014) 35–46.
- [4] Maldague, X., Marinetti, S. Pulse phase infrared thermography. *J. Appl. Phys.*, 79 (1996), pp. 2694–2698
- [5] Monte, C. and Hollandt, J. The Measurement of Directional Spectral Emissivity in the Temperature Range from 80 °C to 400 °C at the Physikalisch-Technische Bundesanstalt. *High Temperatures - High Pressures*, 39, (2010), 151-164